Numerical modelling of offshore pile driving

Pop, C.; Zania, Varvara; Trimoreau, B.

Published in:
Proceedings of XVI European Conference on Soil Mechanics and Geotechnical Engineering

Publication date:
2015

Document Version
Peer reviewed version

Numerical modelling of offshore pile driving

Modélisation numérique de battage de pieux en mer

C. Pop[1], V. Zania[*2] and B. Trimoreau[3]

[1] *Technical University of Denmark , Copenhagen, Denmark*
[2] *Technical University of Denmark, Copenhagen, Denmark*
[3] *Lloyd' s Register Consulting, Copenhagen, Denmark*
[*] *Corresponding Author*

ABSTRACT The number of offshore pile driving activities is increasing, following the growth of offshore wind farms in European waters. The most popular deep foundation employed at present for offshore turbines is the monopile that is driven into the seabed. The installation of these large diameter steel piles is achieved by using hydraulic hammers and applying enormous impact energy. Pile driving generates high-pressure acoustic waves in the surrounding water and sediments and therefore, environmental concerns in connection with marine life have been raised. Noise regulations are in place in German waters, so the necessity to predict and model noise propagation has arisen to optimize mitigation measures. The underwater noise that is produced during pile driving is mostly due to a radial expansion wave propagating along the pile after impact that generates conical acoustic wavefronts in the surroundings. The current study aims at investigating the dynamic pile-water-soil system by means of finite element modelling. The loss mechanisms experienced by the structural waves at the pile-sediment interface and by the body waves in the soil need to be accounted for to accurately estimate the received acoustic waves in the water. Axisymmetric finite element models are developed where the soil is considered homogeneous continuum with linear elastic material behaviour. Appropriate boundary conditions are also implemented in order to treat the semi-infinite domains of both water and soil, thus to avoid any spurious wave reflections at the boundaries. The effect of various soil conditions is investigated through a parametric study.

RÉSUMÉ Le nombre d'activités de battage de pieux en mer augmente, en lien avec la croissance du secteur éolien offshore en Europe. Le type de fondation le plus répandu à présent est le monopieu, qui est enfoncé dans le sol. L'installation de ces pieux d'acier de large diamètre est réalisée à l'aide de marteaux hydrauliques exerçant une forte énergie d'impact. Le battage génère l'émission de forte puissance d'ondes acoustiques dans l'eau et le sol environnants, et donc des préoccupations environnementales sur la faune marine ont émergé. Des réglementations de bruit sont en vigueur dans les eaux allemandes accélérant la nécessité de modéliser la propagation sonore afin d'optimiser les mesures d'atténuation du bruit. Le bruit sous-marin lors du battage est principalement causé par une expansion radiale se propageant le long du pieu après l'impact, et générant des ondes acoustiques coniques dans les environs. La présente étude vise à examiner le système dynamique pieu-eau-sol à l'aide de la méthode des éléments finis. Les mécanismes de pertes - subies par les ondes structurelles à l'interface pieu-sol et par les ondes de corps dans le sol - sont pris en compte, afin d'estimer précisément les niveaux sonores reçus dans l'eau. Des modèles axisymétriques d'éléments finis sont développés dans lequel le sol est considéré homogène ayant un comportant linéaire élastique. D'adéquates conditions aux limites sont implémentées pour traiter les domaines semi-infinis de l'eau et du sol, pour assurer la continuité de propagation. Les effets de différentes conditions de sol sont examinés à travers une étude paramétrique.

1 INTRODUCTION

The most popular deep foundations of offshore wind turbines so far are large diameter (2-7m) steel monopiles, driven in the seabed by impact. The released energy during impact is transformed to high-pressure acoustic (compression) waves in the surrounding air, water and soil sediment which generate underwater noise (Reinhall & Dahl 2011). Concerns on the negative environmental impact of underwater noise related mainly to the marine mammals have been raised. Thereafter extensive monitoring programs have been implemented during the construction and operational period of offshore wind farms. Nonetheless noise regulations are already in place in German waters through the BSH guidelines for certification of offshore wind farms (Müller & Zerbs 2011). Therefore along with the growth of offshore wind farms, the necessity to predict and model underwater noise has arisen.

The radial oscillations of the pile wall generated due to the Poisson's effect by the compression wave after the impact is the main source of the acoustic waves within the water (Reinhall & Dahl 2011).

However three main transmission paths have been identified: (a) the direct pile-water path, (b) the indirect pile-soil-water path, and (c) the indirect pile-air-water path which is often disregarded due to its minor contribution (Lippert et al. 2013). A realistic estimation of the underwater noise levels requires efficient modelling of the two major transmission paths, hence pile-water interaction, pile-soil interaction, water-soil coupling and wave propagation within the soil medium.

The numerical methods available in the literature to analyse pile driving can be classified as: (a) lumped parameter models (Smith 1960, and Randolph 2003), (b) continuum finite element models (Masouleh & Fakharian 2007; Masoumi et al. 2007), and (c) acoustic finite element models (Reinhall & Dahl 2011; Milatz et al. 2012).The drawbacks of the abovementioned methods can be summarized as: (a) lumped parameter models do not account for the water medium, the coupling effect between the water and seabed, and the propagation of non plane strain waves within the soil, (b) continuum finite element models disregard usually the water medium, therefore underwater noise estimation is not possible, (c) acoustic finite element models do not capture phenomena such as bottom loss due to the acoustic wave propagation in the water, interface wave generation at the water-seabed boundary, energy dissipation via hysteretic damping, since the soil constitutive behaviour is simplified to equivalent fluid.

In the current study a hybrid (acoustic for the water domain and continuum for the soil domain) near-field (up to 80m from the shaft) complete interaction model is developed, capturing wave propagation along the two major transmission paths. The approach is compared to the corresponding acoustic finite element model in order to highlight the limitations of the latter. A parametric study is conducted to investigate the role of the soil stiffness on the hydro-acoustic pressure.

2 METHODOLOGY

The hybrid finite element model developed in the current study to investigate the acoustic radiation due to impact driving is shown in Figure 1. Axisymmetric modelling is employed and the explicit integration solver of the commercial software Abaqus is used for the analysis. The explicit time integration is chosen due to the reduction of computational cost.

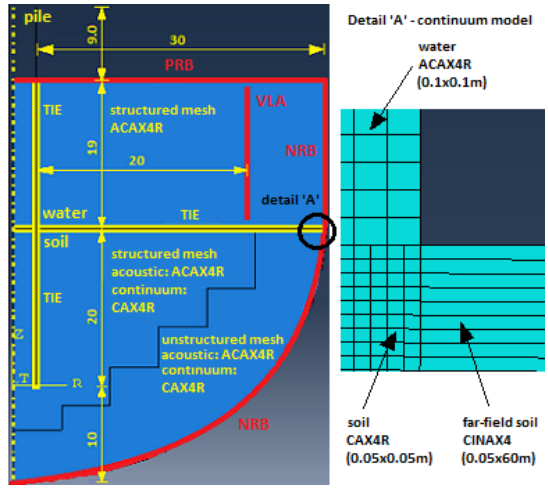

Figure 1. Finite element model geometry, meshing and boundary conditions.

The mesh size for each domain of the model is established based on the minimum wave speed characterizing the material (c_{min}) and the maximum exciting frequency (f_{max}) that needs to be captured, such as at least six elements per wavelength are provided (Milatz et al. 2012). An equivalent acoustic model is also developed, where the soil is modelled as fluid. The type and element size of the two finite element models is depicted in Figure 1. The sea surface is modelled as a pressure-release boundary (PRB) due to the almost zero impedance contrast between air and water. The far-field effect of the acoustic media (water and fluid soil) is modelled through improved simple impedance boundaries (non-reflecting boundaries – NRB). These boundaries prevent spurious wave reflections at the media edges for any incidence angle. In the continuum approach the far-field effect of the soil is modelled using infinite elements (CINAX4) which are non-reflecting boundaries as well (Figure 1). The load function applied at the pile head as a pressure load to simulate the hammer impact has been selected as in other studies in the literature (Zampolli et al. 2013) (Figure 2).

The sound speed profile within the fluid domain is assumed constant. The water density is set as 1024kg/m^3, while the sound speed as 1480m/s.

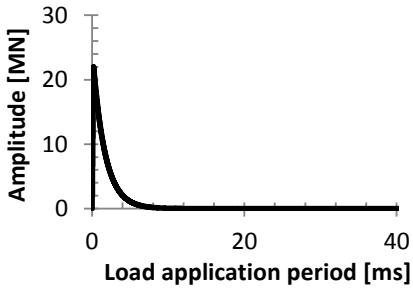

Figure 2. Load function used for simulating the hammer impact.

The soil is considered a homogeneous continuum medium with linear elastic material behaviour. In the hybrid model, the linear elastic soil is characterised by Poisson's ratio, ν_s, Young's modulus, E_s and the material density, ρ_s. The compressional or P-wave velocity is determined as function of the saturation (Verruijt 2005). Saturated soils attain higher compressional wave speed, than dry soils, due to the increase in volumetric stiffness by the pore water. Since the soil is assumed here to be saturated but is modelled as a continuum and not two phase material, the pore water cannot be accounted for directly in the numerical model. Thus, for obtaining the same c_p as for the fluid soil, the elastic parameters (ν_s and E_s) are calibrated to derive the correct shear and compressional wave velocities (c_p and c_s) within the soil (see Table 1).

For direct comparison of the wave propagation in the acoustic (model 1) and the hybrid (model 2) models, the soil is initially considered to be stiff, with c_s=400m/s. The effect of different soil conditions (softer soils) on the wave propagation in the water and soil domains is investigated later on by a parametric study (models 3 and 4). The geometry and material properties of the steel monopile are the kept constant throughout the current investigation (ρ_p=7800kg/m^3, E_p=207x10^{9}Pa, ν_p=0.3). The pile dimensions are: 48m length, 4.8m diameter and 0.05m wall thickness. Displacement compatibility between the different domains of the model (pile, water, soil) is materialized by tied constraints at the common interfaces. Therefore, at the pile-soil interface, no slip can occur between the two parts. Thus, the energy dissipation at the pile shaft through interface friction is not considered in this model. An analysis of the single pile to impact is also performed.

Table 1. Stiffness properties for the soil domain

Model no.	Soil stiffness	ρ [kg/m^3]	c_p [m/s]	c_s [m/s]
1	acoustic	1900	1700	0
2	stiff	1900	1700	400
3	medium	1900	1700	200
4	soft	1900	1700	50

3 WAVE PROPAGATION ANALYSIS

3.1 Wave propagation in the pile

The soil shear stiffness effect on the wave propagation in the pile is observed by plotting the axial stress time history for a point on the pile 7.0m below seafloor in three cases: single pile rigidly supported at the tip, model 1 and model 2 (Figure 3).

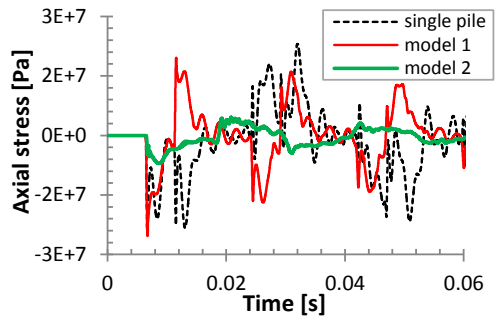

Figure 3. Axial stress time history in the pile 7.0m below seafloor.

The first peak amplitudes – which represent the initial downward compressive wave – are equal only for the first two cases, i.e. single pile and model 1. In model 2 a significant amplitude decrease is observed for the first peak. At this location, the initial stress wave has already travelled 7.0m in the embedded part of the pile. Consequently, the amplitude reduction for the first peak – compared to the other two cases- is caused by the axial strain reduction due to the soil shear stiffness encountered along the propagation over the embedded first 7.0m. The soil shear stiffness causes a resistance against the development of the axial strains, thus a reduction in the axial stress amplitude. In model 2, there is also a delay in the wave arrival time compared to the other two models, which is also attributed to the soil shear stiffness.

3.2 Wave propagation in the acoustic model

Since the compression wave travels faster in the pile (c_p=5151m/s) than in the water (c_p=1480m/s) or the fluid seabed (c_p=1700m/s), the primary spherical wave fronts produced by the oscillation of each point on the pile will overlap (Heitmann et al. 2013). Due to the time lag between the emissions of consecutive spherical fronts, there will also be a difference in the volume covered which leads to the final acoustic field with conical shape. The conical field observed in other studies (Reinhall & Dahl 2011; Heitmann et al. 2013), is captured in model 1 as well as shown by the hydroacoustic pressure contour snapshots shown in Figure 4. The compressive nature of the first downward propagating wave in the pile causes the first acoustic front to be compressive as well, as it can be seen in the snapshot at 9.0ms. The subsequent wave fronts belong to the first downward propagating cone, visible in the same screenshot, and alternate in phase as they are caused by the pile wall oscillations after the initial wave has passed.

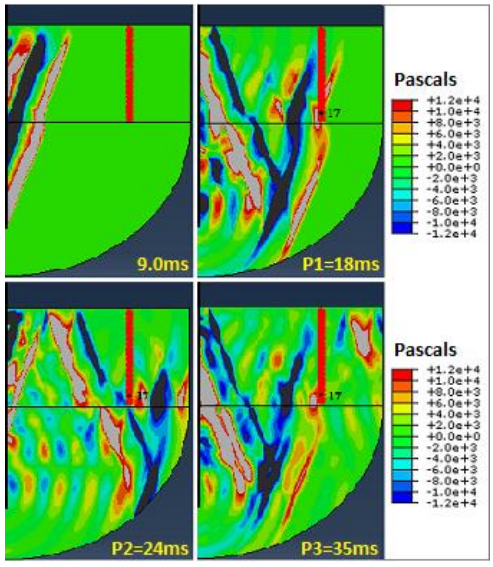

Figure 4. Hydroacoustic pressure contours snapshots. The wave fronts in model 1 are shown.

3.3 Wave propagation in the continuum model

Pile-driving induces P-waves in the soil caused as in the acoustic approach by the radial expansion wave in the pile and vertically polarized shear waves caused by the shear deformation induced at the shaft during driving. This is visible as the pressure stress (P-waves) and deviatoric stress (S-waves) contour plots at Figure 5.

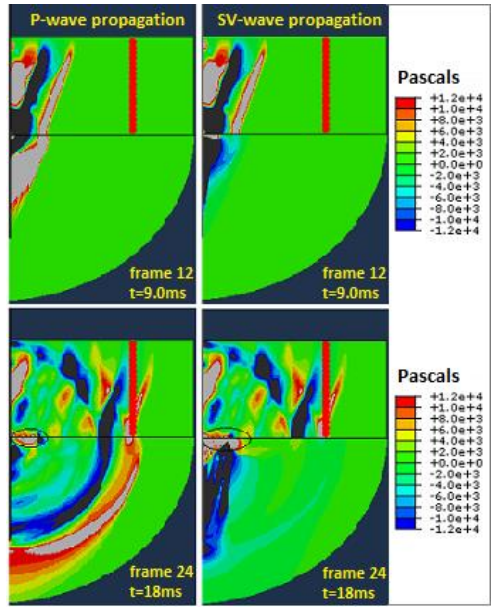

Figure 5. Pressure and deviatoric stress contour plots depict the P and SV-wave front propagations respectively in model 2.

It has been observed that until at least a distance from the shaft equal to the embedded depth of the pile and for this magnitude of shear stiffness, the shear waves propagating on a cylindrical front dominate the propagation around the shaft. This aspect has been observed in other studies as well (Masoumi et al. 2007). Stress concentration areas have been identified at the water-soil interface visible at time equal to 18ms in the contour plots showing the P and SV-wave front propagations (Figure 5). This is attributed to generation of interface Scholte waves which contain both P and SV components and occur at the boundary between a fluid and solid, due to the discontinuity in shear stresses at this location. The Scholte wave speed determined using the analytical solution (Dong & Hovem 2011) yielded similar value to the one estimated from the numerical solution ($v_{scholte}$=354m/s), which supports the fact that the wave observed at the water-soil interface is indeed the Scholte wave. The numerical wave speed has been estimated after the wave arrival time, detected

by plotting a synthetic seismogram of the P-wave component (Figure 6).

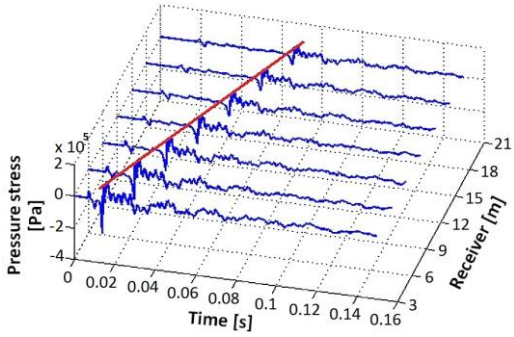

Figure 6. Synthetic seismogram of P-wave component for detecting the interface Scholte wave.

3.4 Hydroacoustic pressure variations

In order to highlight the differences between the acoustic and the continuum soil modelling, the acoustic pressure variation is plotted 20m from the shaft and 2.0m above the seabed (Figure 7).

In the acoustic model, a clear phase division representing the downward and upward propagating cones can be observed. Phase 1 (P1) captures the first three wave fronts belonging to the initial downward propagating cone in the water (Figure 4 – 18ms). This phase is naturally captured in the hybrid model as well. However, a decrease can be observed in the third peak's amplitude. This occurs since the third front experiences the additional bottom loss mechanisms associated with the shear waves. The soil shear stiffness represents an additional degree of freedom for the acoustic wave to penetrate into the soil (shear wave conversion). Thus, the energy loss experienced by the acoustic waves in the water at the seafloor level is represented in the hybrid model.

In model 1, P3 (Figure 4 – 35ms) and P5 are a repetition of P1, being caused by the second and third downward propagating cones. P2 (Figure 4 – 24ms), P4 and P6 are caused by the upward propagating cones after wave reflection occurs at the pile tip. In model 2, the upward cones in the soil and water are not visible for this high level of shear stiffness. This is caused by the significantly decreased radial strains in the pile due to the presence of the soil shear stiffness. For this reason, the hydroacoustic pressure from the direct pile-water path is decreased as well.

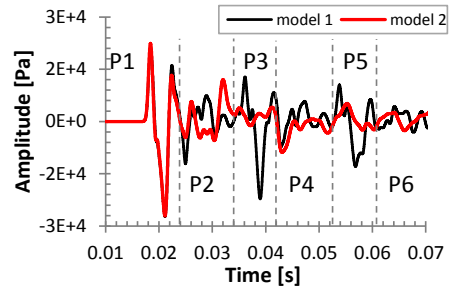

Figure 7. Comparison of the hydroacoustic pressure time histories obtained

4 PARAMETRIC STUDY

The soil shear stiffness plays a fundamental role in the wave propagation, bottom loss and acoustic pressure generation within the complete interaction model. In order to investigate the effect of the soil shear stiffness, models 3 and 4 are analysed (soil properties are listed in Table 1).

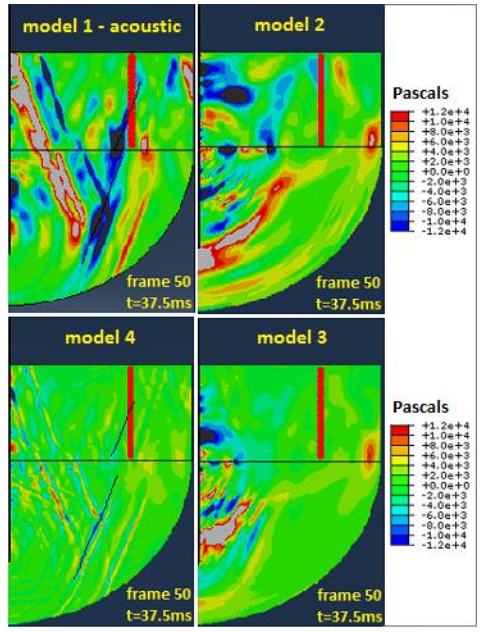

Figure 8. Soil shear stiffness effect on the compressional wave propagation.

Investigating the P wave propagation in the four studied models, it appears that the upward and

downward propagating cones in both water and soil media are clearly distinguishable in model 4, similarly to model 1 (Figure 8), but with reduced amplitude due to the decrease in axial strains in the pile because of the small, but present soil shear stiffness. On the contrary, for the stiffer soils (models 2 and 3) the pressure cones do not develop anymore.

Another observation of the parametric study is that for soils with considerable shear stiffness ($c_s \geq 200$m/s), the shear waves dominate the propagation around the shaft, while in the case of soft soils the propagation is dominated by compression waves. Hence, the acoustic modelling approach may represent a fair approximation of the wave propagation for very soft soils. The Scholte wave penetration depth into the water is investigated for models 2 and 3 through penetration envelopes that describe the penetrations of a wave in a certain location at subsequent times (Figure 9). By comparing the two envelopes, it appears that the penetration into the water increases with increasing soil shear stiffness. This effect has been observed in one recent study as well (Tsouvalas & Metrikine 2014). Comparing the acoustic pressure amplitudes along the penetration in the two models, it is evident that the energy carried by the Scholte wave in the water increases with increasing soil shear stiffness. Consequently, the hydroacoustic pressure close to the seafloor is likely to contain Scholte wave energy and affect the underwater noise.

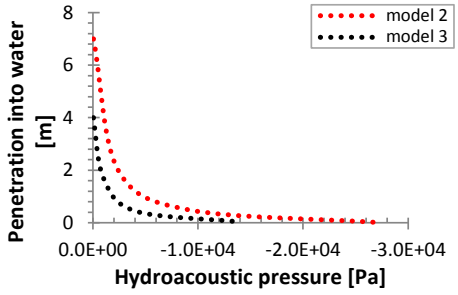

Figure 9. Variation of Scholte wave penetration into the water medium with soil shear stiffness

5 CONCLUSIONS

In the study, a hybrid finite element model has been developed to investigate the wave propagation in the complete pile-soil-water interaction system. The numerical model was able to capture the full wave propagation in both the water and soil media, including the vertically polarized shear waves in the soil, the Scholte waves at the seafloor, as well as different energy loss mechanisms that affect the total hydroacoustic pressure. The effect of the soil stiffness on the wave propagation has been examined and it was observed that the acoustic model gives a fair approximation of the wave propagation for very soft soils.

REFERENCES

Dong, H. & Hovem, J.M. 2011. *Interface Waves, Waves in Fluids and Solid*, Prof. Ruben Pico Vila (Ed.) InTech, Rijeka.

Heitmann, K. Lippert, T. Lippert, S. Ruhnau, M. & von Estorff, O. 2013. On the prediction of pile driving induced underwater sound pressure levels over long ranges. *Proceedings, 20th International Congress on Sound & Vibration, ICSV20,-*. ICSV, Bangkok.

Lippert, S. Lippert, T. Heitmann, K. & Von Estorff, O. 2013. Prediction of underwater noise and far field propagation due to pile driving for offshore wind farms. *Proceedings of Meetings on Acoustics, ICA 2013 Montreal,-*. ICA, Montreal.

Masouleh, S.F. & Fakharian, K. 2007. Application of a continuum numerical model for pile driving analysis and comparison with a real case. *Computers and Geotechnics* **35,** 406-418.

Masoumi, H.R. Degrande, G. & Lombaert, G. 2007. Prediction of free field vibrations due to pile driving using a dynamic soil-structure interaction formulation. *Soil Dynamics and Earthquake Engineering* **27,** 126-143.

Milatz, M. Lippert, S. Lippert, T. Von Estorff, O. & Reimann, K. 2012. Prediction of underwater sound due to pile driving for offshore wind farms – a challenge for numerical simulation. *Proceedings, 41st International Congress and Exposition on Noise Control Engineering*, 7939-7950. Inter.noise, New York City.

Müller, A. & Zerbs, C. 2011. *Offshore wind farms measuring instruction for underwater sound monitoring*. Report by BSH, 1-31.

Randolph, M.F. 2003. Science and empiricism in pile foundation design. *Géotechnique* **53,** 847-875.

Reinhall, P.G. & Dahl, P.H. 2011. Underwater Mach wave radiation from impact pile driving: Theory and observation. *Journal of the Acoustic Society of America* **130,** 1209-1216.

Smith, E.A.L. 1960. Pile-driving analysis by the wave equation. *Journal of the Soil Mechanics and Foundations Division* **86,** 35-61.

Tsouvalas, A. & Metrikine, A.V. 2014. A three-dimensional vibroacoustic model for the prediction of underwater noise from offshore pile driving. *Journal of Sound and Vibration* **333,** 2283-2311.

Verruijt, A. 2005. *Soil Dynamics*, Delft University of Technology, Zoetermeer.

Zampolli, M. Nijhof, M.J.J. De Jong, C.A.F. Ainslie, M.A. Jansen, E.H.W. & Quesson, B.A.J. 2013. Validation of finite element computations for the quantitative prediction of underwater noise from impact pile driving. *Journal of Acoustic Society of America* **133** (1), 72-81.